Multidecadal elevation changes from spy satellite images: application to glaciers and landslide

Amaury Dehecq[1,2,3], Alex Gardner[3], Oleg Alexandrov[4], Scott McMichael[4], Romain Hugonnet[5], David Shean[6], Mauro Marty[2], Pascal Lacroix[7]

1. Laboratory of Hydraulics, Hydrology and Glaciology (VAW), ETH Zurich, Zurich, Switzerland.
2. Swiss Federal Institute for Forest, Snow and Landscape Research (WSL), Birmensdorf, Switzerland.
3. NASA Jet Propulsion Laboratory, California Institute of Technology, Pasadena, CA 91109, USA
4. NASA Ames Research Center, Moffet Field, CA 94035, USA
5. LEGOS, Université de Toulouse, CNES, CNRS, IRD, UPS, F-31400 Toulouse, France
6. Civil and Environmental Engineering, University of Washington, Seattle, WA, United States
7. ISTerre - Université Grenoble Alpes, IRD, CNRS, IFSTTAR, Université Savoie Mont Blanc, Grenoble, France

I. Intro - Context

- Earth's surface changed dramatically over the past century
- Publicly available, high resolution, satellite imagery is lacking prior to ~2000 to study such changes at multi-decadal time scales
- American declassified satellite images could fill in the gap! … but processing is challenging.

Example of Columbia glacier, Alaska

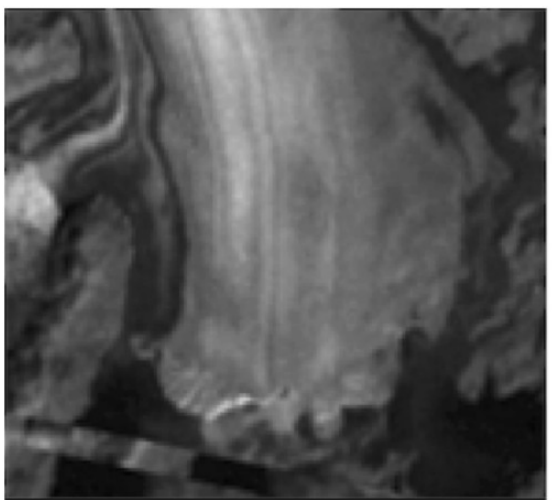

Landsat 3 1979/09/07
Pixel size: 60 m

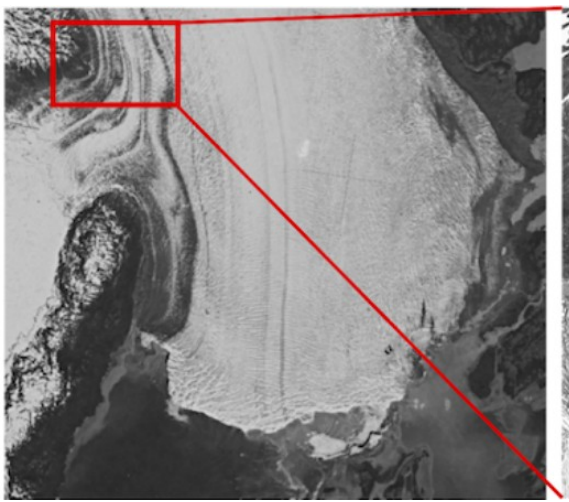

Hexagon (mapping) 1979/06/15
~6 m

Hexagon (pano) 1980/08/23
~0.6 m

I. Intro - US “spy” programs

- 1959-1972 - Corona (KH-1-6) series - 1.8-7.5 m resolution
- 1963-1984 - Gambit (KH-7-8) series - Up to 0.1 m
- **1973-1986 - Hexagon (KH-9) series -** 0.6 m (pano camera), **6 m (mapping camera)**

We focus on this data set

=> Available on USGS https://earthexplorer.usgs.gov/ (‘Declassified Data’ data set)

  - Hexagon mapping camera : **29 000 images** (~4000 already scanned)
  - All US spy satellites : 2 million (stereo) images over 20 years !

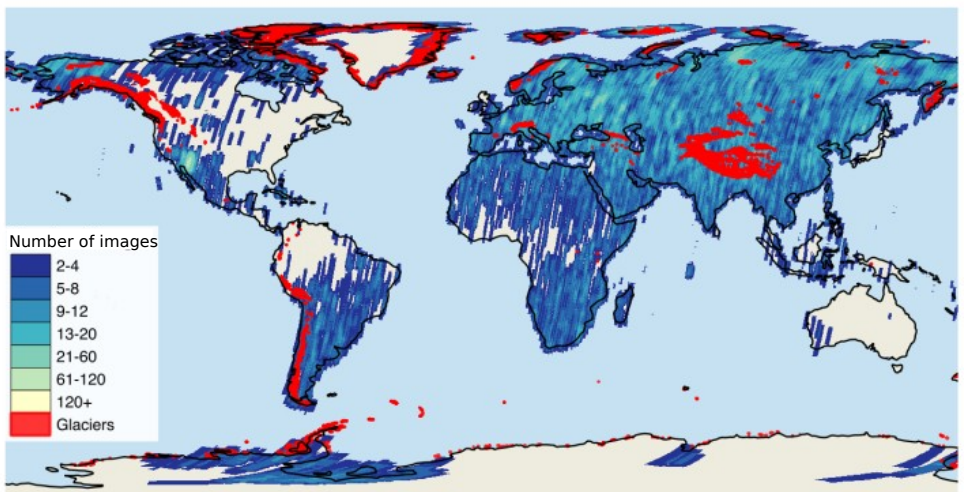

KH-9 mapping camera

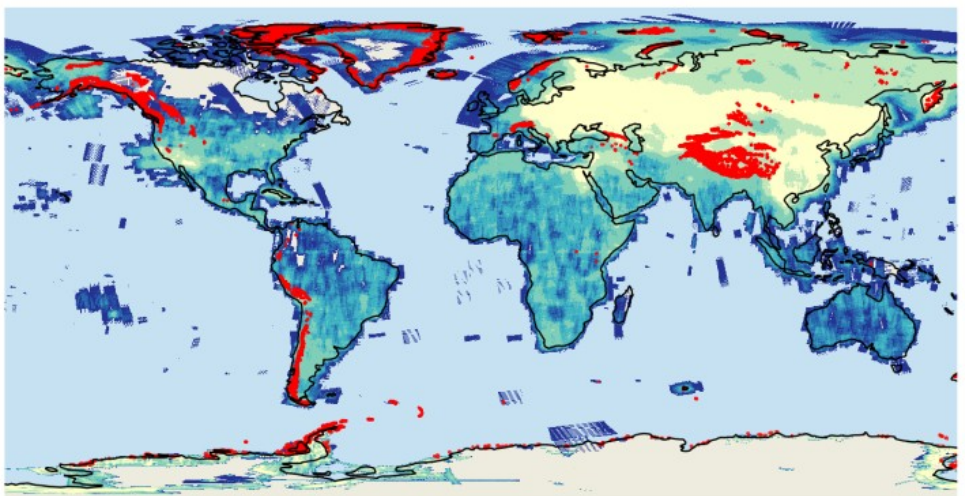

All other US “spy” satellites

I. Intro - The Hexagon (KH-9) program

- 20 missions - 32-176 days duration
- main payload : 2 panoramic cameras - 0.6 m resolution
- 12/20 included a frame **mapping camera (MC)** - 6-9 m resolution
- Photo printed on film → 4 re-entry capsules ("buckets") snatched mid-air

KH-9 vehicle

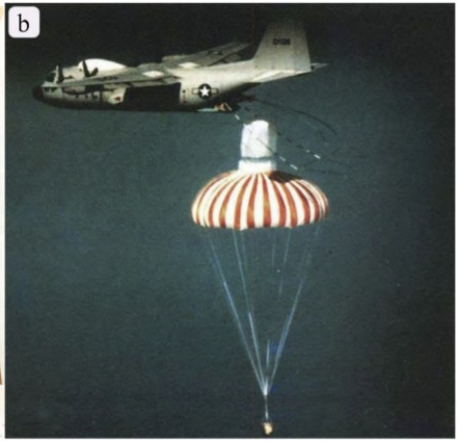

Aerial recovery of the film (Maurer et al. (2015))

~260 km / 46 cm = 66K pixels

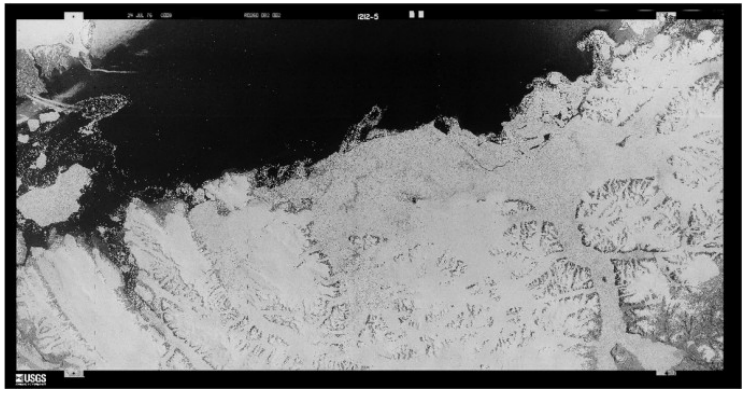

Example of a KH-9 MC film (46 x 23 cm^2) over the Canadian Arctic

More info:
- Burnett et al. (2012)
- Aizen & Surazakov (2010)
- Maurer et al. (2015)

Challenges:
- Large (~ 2 GB) images scanned in **2 pieces + film distortion** → heavy preprocessing
- Images **crudely geolocated**, no ground control points available
- Satellite position + lens characteristics poorly known or classified

I. Intro – Overview of the workflow

A preprocessing workflow: from scans to undistorted/croppped image

- Fully automated in Python (scikit, OpenCV libraries)
- ~1 hour to process one image on 1 core

→ Applied to ~700 images with less than 10 failures

A stereo processing: from stereo pairs to DEM + orthoimage

- Python wrappers around the NASA Ames Stereo Pipeline (link)
- Processing at ½ resolution → estimate camera intrinsic parameters

→ Applied to ~400 higher quality images to derive focal length & lens distortion for each mission

- Processing at full resolution with estimated parameters

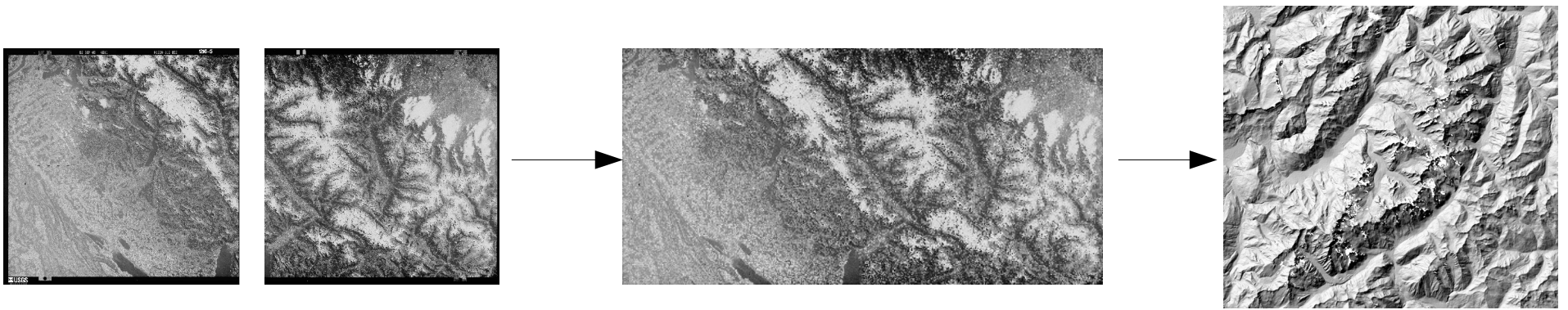

Scanned film pieces

Undistorted digital image

Regional DEM

II. Preprocessing - Methods

Goal: Generate distortion-free images suitable for photogrammetry.

Preprocessing similar to that of Maurer et al. (2015), tuned and tested on ~700 images with varying conditions (deserts, ice caps, oceans...):

- **Correction of distortion:** **(1)** Detection of the 1081 fiducial markers (crosses) **(2)** Interpolation of the distortion in each pixel and correction.
- **Image stitching :** **(1)** The left/right image pieces are stitched together using interest-point matching (SIFT) in area of overlap. **(2)** Image is cropped to remove dark bands around the film.

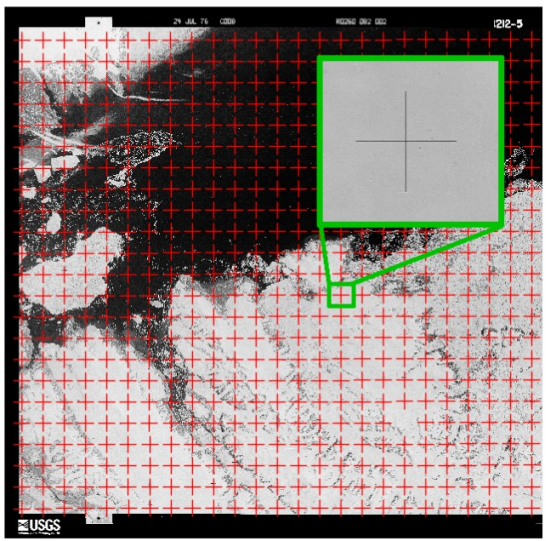

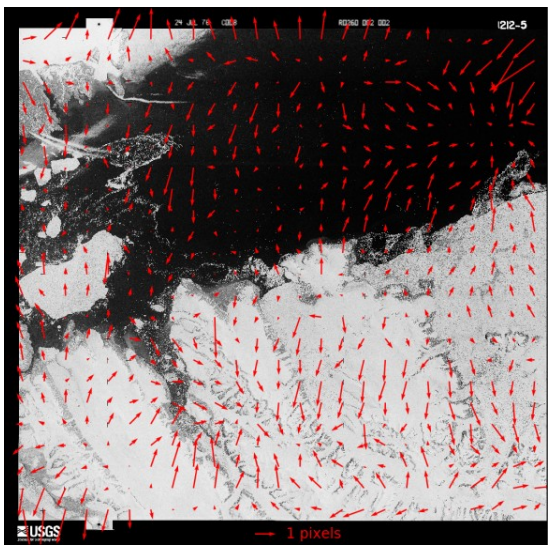

Identification of the fiducial markers (left) and estimated film distortion (right), after removal of a rotation/scaling.

II. Preprocessing - Results

The mean distortion from ~1400 image halves reveals systematic distortions:

A **rotation and/or scaling,** likely introduced during scanning – 3 markers are necessary to correct these.

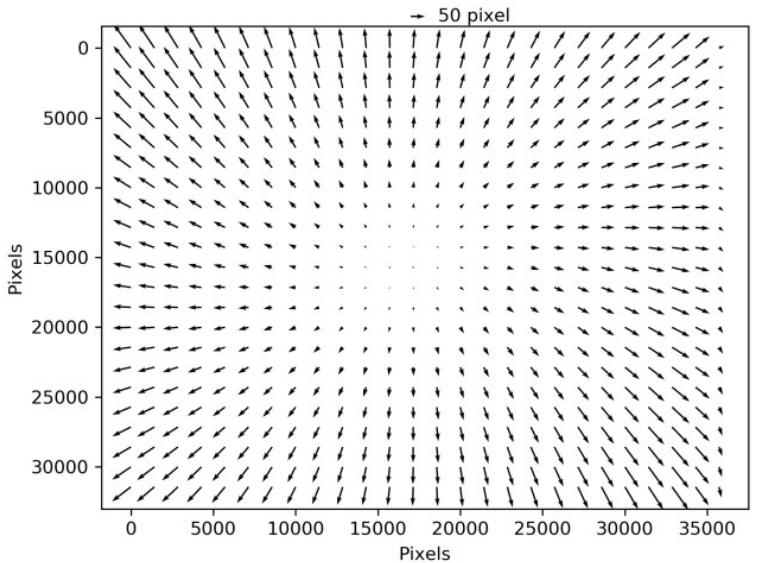

After rotation/scaling correction, residual distortions of a few pixels (1 pix=7µm) is present, with **a shear pattern**, likely caused by the film advancing mechanism (on orbit and during scanning) – Only a *réseau* grid and thorough preprocessing can correct this.

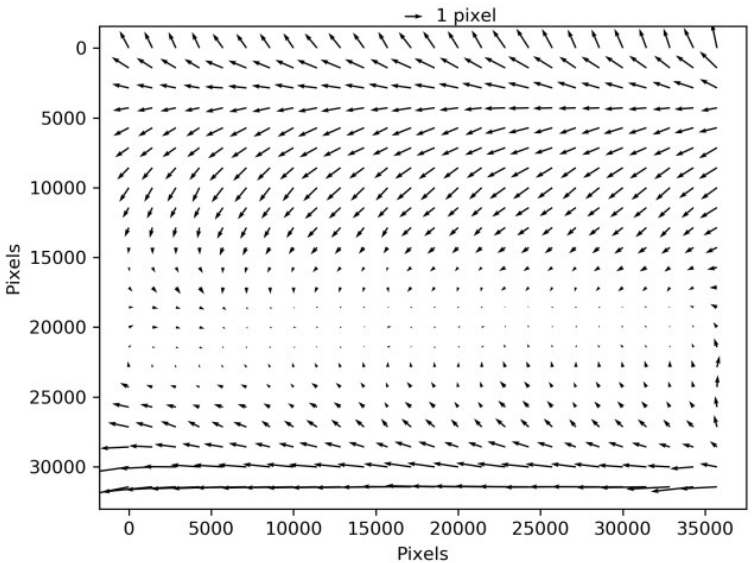

III. Stereo processing - Methods

From stereo pairs, we generate Digital Elevation Models (DEMs) using the open-source **NASA Ames Stereo Pipeline** (*Shean et al., 2016*).

Challenges:
- Images are very crudely geolocated, no existing Ground Control Points (GCPs)
- Satellite position and lens characteristics are unknown/classified.

Estimating the camera model: intrinsic + extrinsic parameters

(1) A pinhole camera model is created (documented focal length 304.8 mm, principal point at center) and its initial position/orientation are estimated from the image footprint provided by USGS.

(2) An initial DEM is generated with these cameras, at 1/2 resolution, then coregistered with a reference DEM (e.g. SRTM), using interest point matching between the shaded DEMs. The camera poses are updated.

(3) Several thousand “GCPs” are extracted, from the dense point-matching and external DEM, and used in bundle adjustment to refine the camera intrinsic parameters (focal length, lens distortion) for all pairs of each mission.

Final DEM:

(1) The images are orthorectified with an external DEM to reduce the parallax between images. Residual parallax represent elevation changes between the KH-9 acquisition and reference terrain.

(2) A dense point cloud is generated using the Semi-Global Matching algorithm, with 7x7 pixels correlation windows.

(3) A final DEM is generated at 24 m resolution.

III. Stereo processing - Results

With best known camera intrinsic parameters, elevation **biases of ±20 m** are present in KH-9 DEMs:
- large scale “Bull’s eye” pattern, due to unaccounted lens distortion (left figure, panel a)
- elevation bias correlated with topography, due to errors in the focal length (left figure, b)

By refining the camera intrinsic parameters for each KH-9 mission (5 to 16), we reduce elevation biases to less than 5 m (right figure).

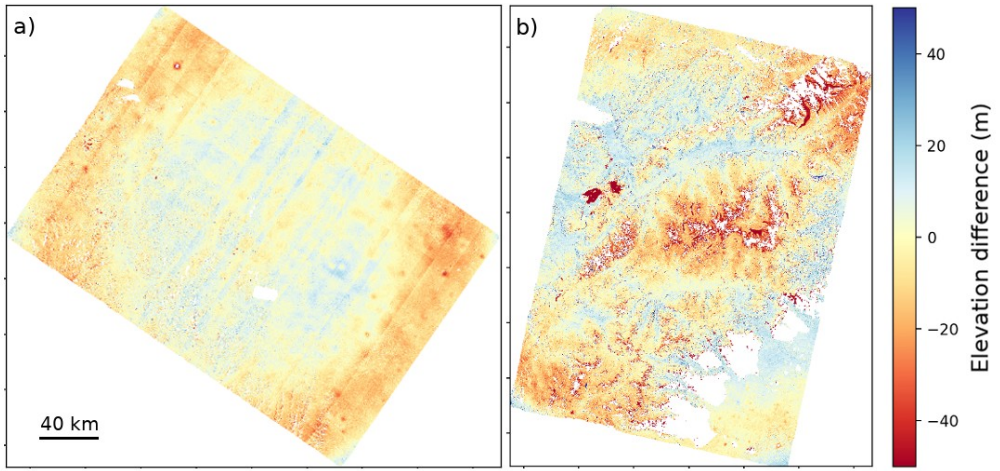

Typical elevation biases before the refinment of camera intrinsic parameters (a) over flat terrains (Alaska) (b) in mountainous areas (central Alps) - mountain ranges are visible in red whereas valleys appear blue.

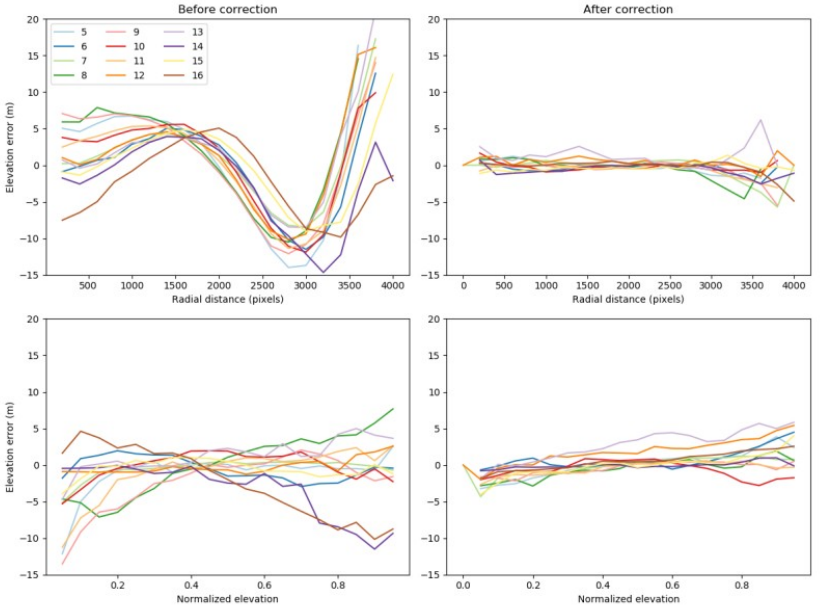

Average elevation error for each KH-9 mission as a function of radial distance to the optical center (top row) and normalized elevation (bottom row), before (left) and after (right) correcting the intrinsic parameters.

IV. Pixel elevation uncertainty

The KH-9 DEMs are validated both **on "stable terrain"** (excluding glaciers) and **on error-prone glacier terrain** in two test regions in South Alaska and in the European Alps. The validation is based on the elevation difference:

- **between overlapping KH-9 DEMs** from same/different orbits (top row).
- **with reference DEMs** (bottom row)

In brief, the **uncertainty is ~5 m at 68%** confidence interval (plain lines), respectively <15 m at 95% (dotted lines).

Note: DEMs obtained from topographic maps ("Hist 1977") show the largest uncertainty (~15 m), highlighting the improved accuracy reached with KH-9 data.

Reference DEMs: SRTM, TanDEM-X, ArcticDEM (*Porter et al. 2018*), the Swiss 2019 topography SwissAlti3D + two historical DEMs in Alaska (1977, *Berthier et al., 2010*) and in the Swiss Alps (1980, *Ginzler et al, 2019*; EGU2020)

European Alps

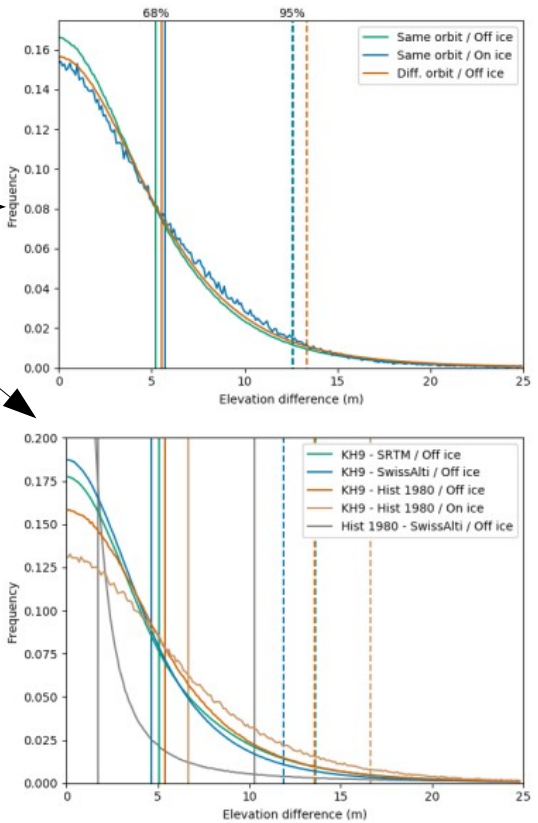

Alaska

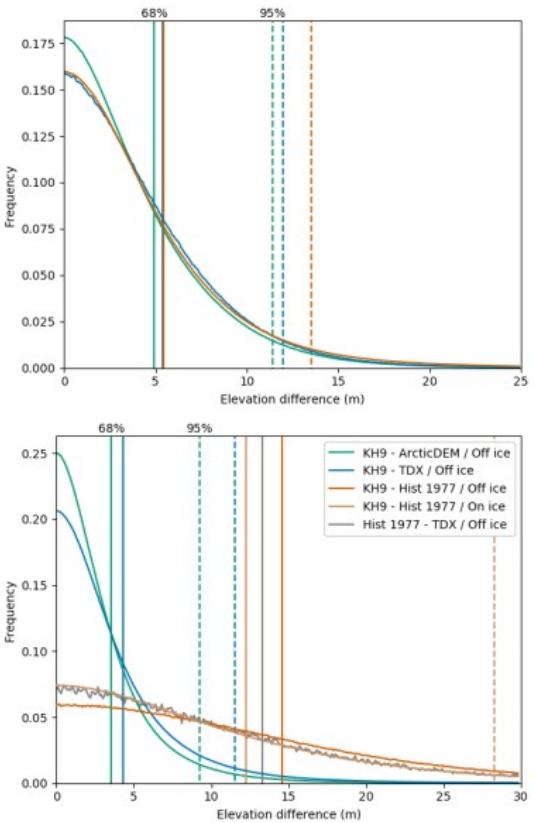

V. Uncertainty on spatial averages - Methods

- Uncertainties can be reduced for spatially averaged elevation changes. For uncorrelated errors, this is the standard error of the mean. For correlated errors (most cases), this requires to know spatial correlation lengths (*Rolstad et al., 2009*).
- Most studies assume a **single correlation length** (~500 m for KH-9, e.g. *Pieczonka et al. (2013)*).
- Using semivariograms (see next slide), calculated on stable terrain from 48 DEMs, we estimate these correlation lengths. Following *Rolstad et al. (2009)*, we calculate the analytical standard error $\sigma_{\Delta h}$, function of the averaging distance L and spatial correlation length a_1 and sill c_1:

$$\sigma^2_{\Delta h} = \begin{cases} c_1 \left[1 - \frac{L}{a_1} + \frac{1}{5} \left(\frac{L}{a_1} \right)^3 \right] & \text{if } L < a_1 \\ \frac{c_1}{5} \left(\frac{a_1}{L} \right)^2 & \text{if } L \geq a_1 \end{cases}$$

(Equation shown here for a single correlation length, but can be summed up for several lengths)

- The results are compared to an empirical estimate, by calculating the standard deviation of average values over “random” patches in stable terrain (e.g. *Miles et al. (2018)*)

V. Uncertainty on spatial averages – Results (1/2)

- The emprical semivariogram (grey dots, left figure) is best fit with **3 spherical models** of spatial correlation length **~0.5, 4 and 60 km** (dotted lines). These lengths correspond to typical “noise” or blunders seen in the elevation change maps (see next slide).
- The analytical error (right figure, orange) agrees well with the empirical error (grey and black lines). Estimates with **single correlation length** of 500 m (resp. 70 km) would **under- (resp. over) estimate the uncertainty**.

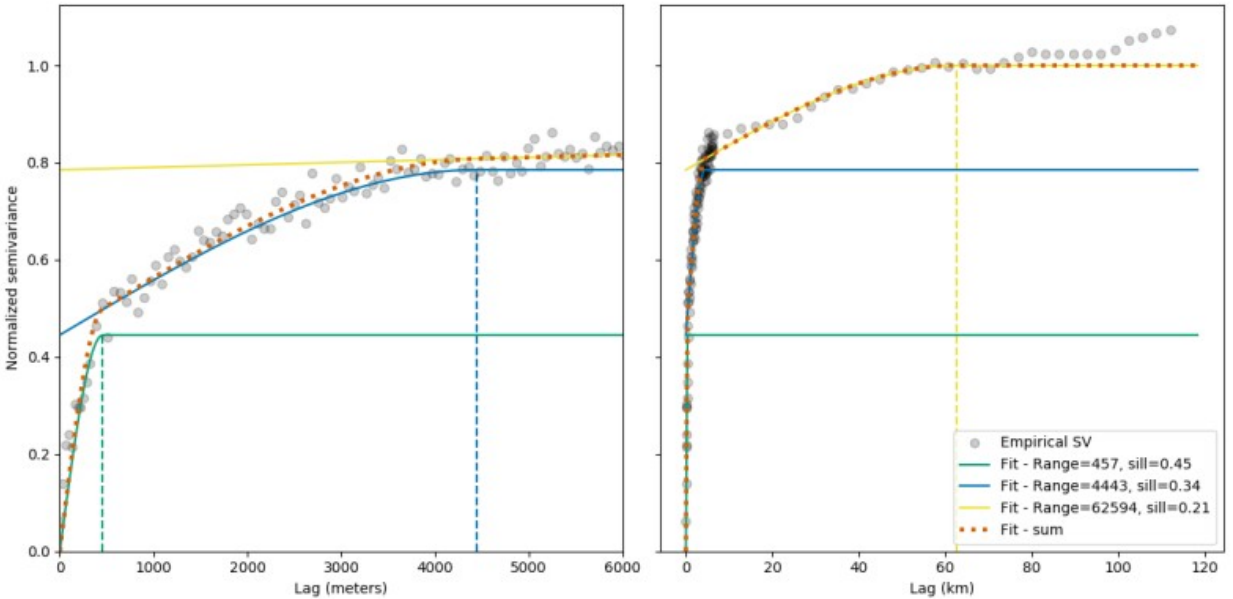

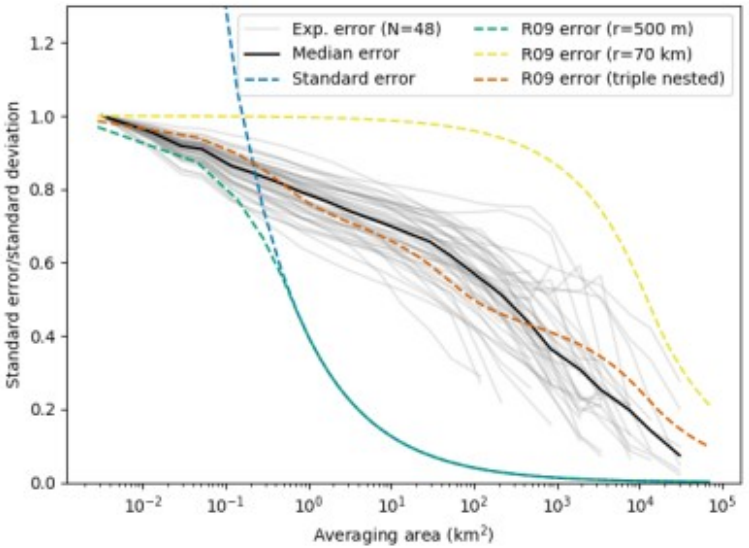

V. Uncertainty on spatial averages – Results (2/2)

Examples of typical errors seen in KH9-derived elevation changes

(here over flat terrain in Alaska)

- Short scale (~500 m → <1 mm on film) noise, probably related to the film grain
- Medium scale (~3-4 km → ~3-4 mm) artifacts, such as bumps, likely caused by dust grain (found at exact same position in consecutive images)
- **Large tiling artifacts.** Assumed to be caused by the scanner, since the size correspond to the size of the CCD sensor of the USGS scanner (Leica DSW700)
- Residuals caused by uncertainties in camera intrinsics parameters, especially near edges

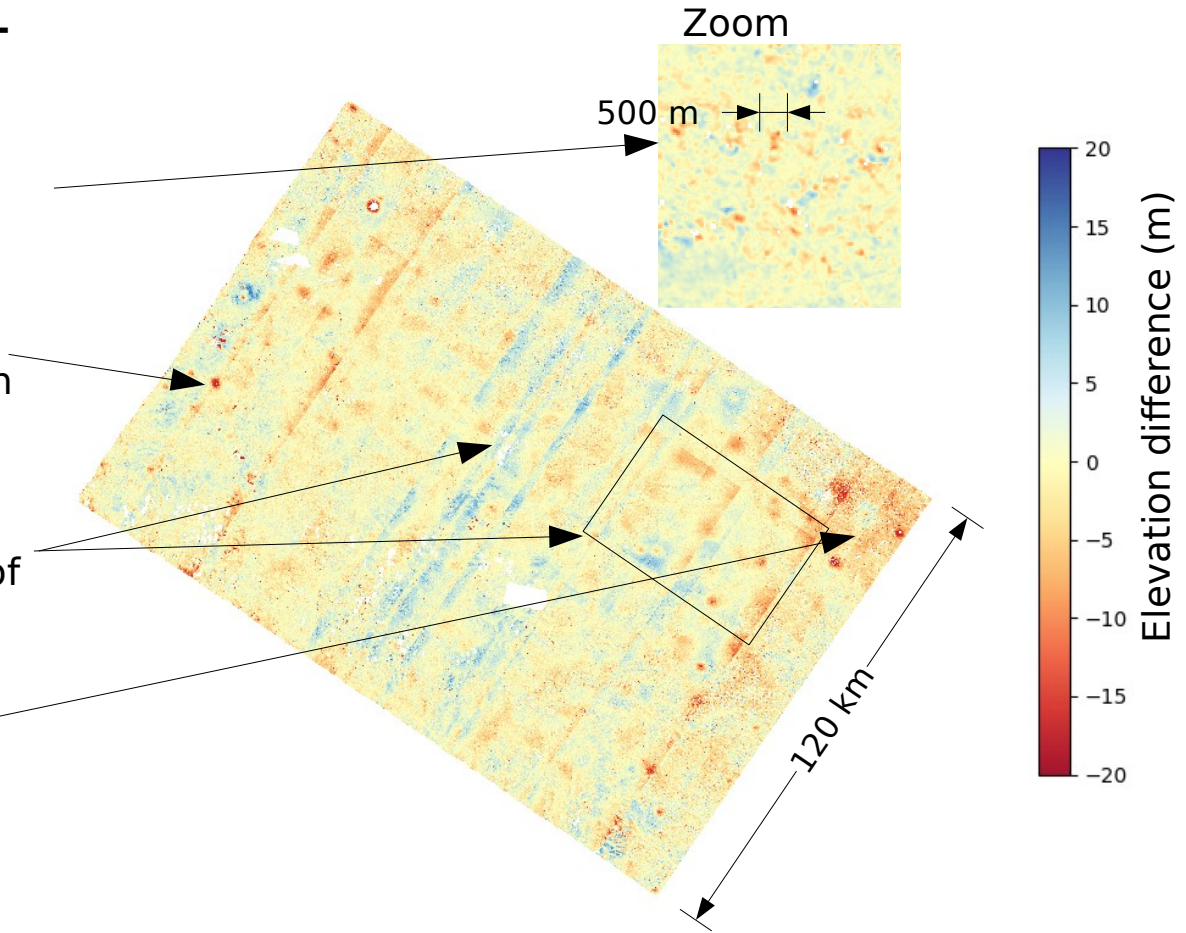

<u>These types of artifacts are expected for other scanned analog images</u>

VI. Applications – Glacier volume changes (1/2)

- We test the **ability to derive accurate glacier volume changes** over the Swiss Alps, where good reference elevation exist both for 1980 (“Hist 1980” aerial DEM) and 2019 (SwissAlti).
- Good agreement between the reference and KH9-derived elevation changes, both in term of spatial and altitudinal distribution, even in snow-covered high altitude areas with little image contrast.

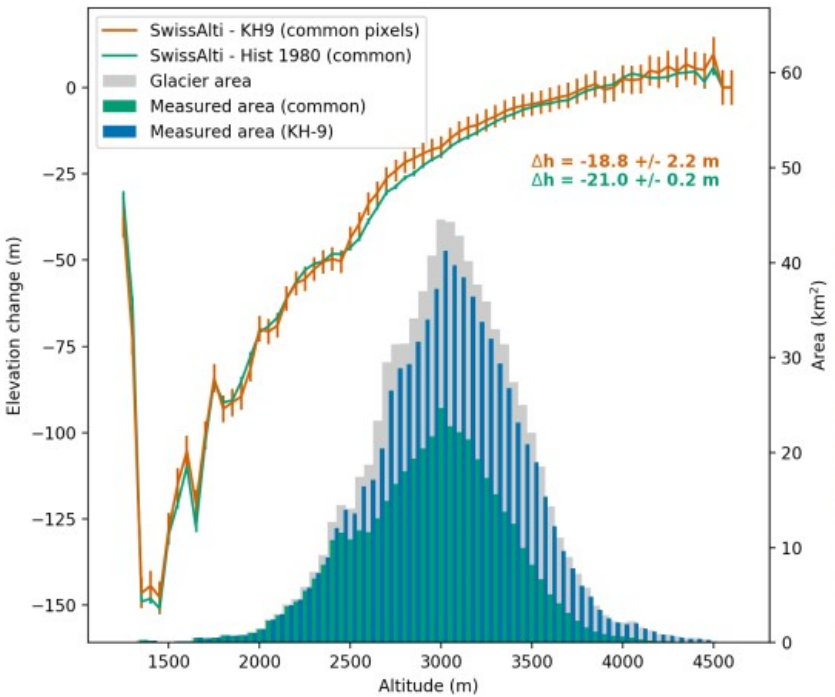

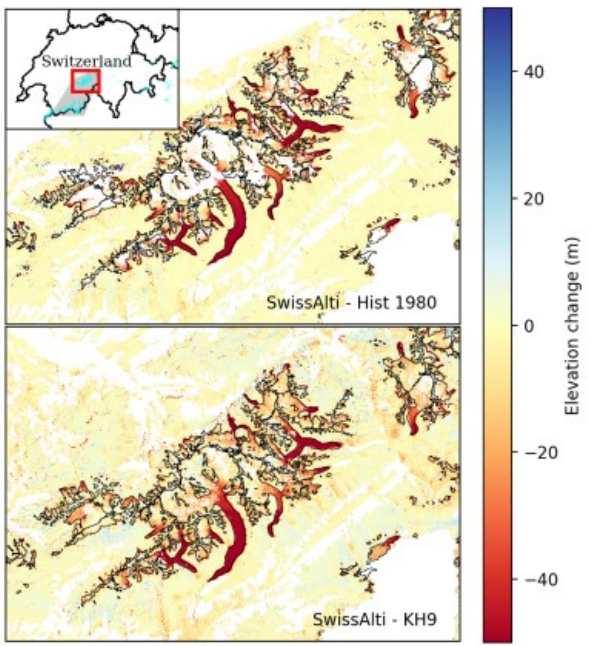

VI. Applications – Glacier volume changes (2/2)

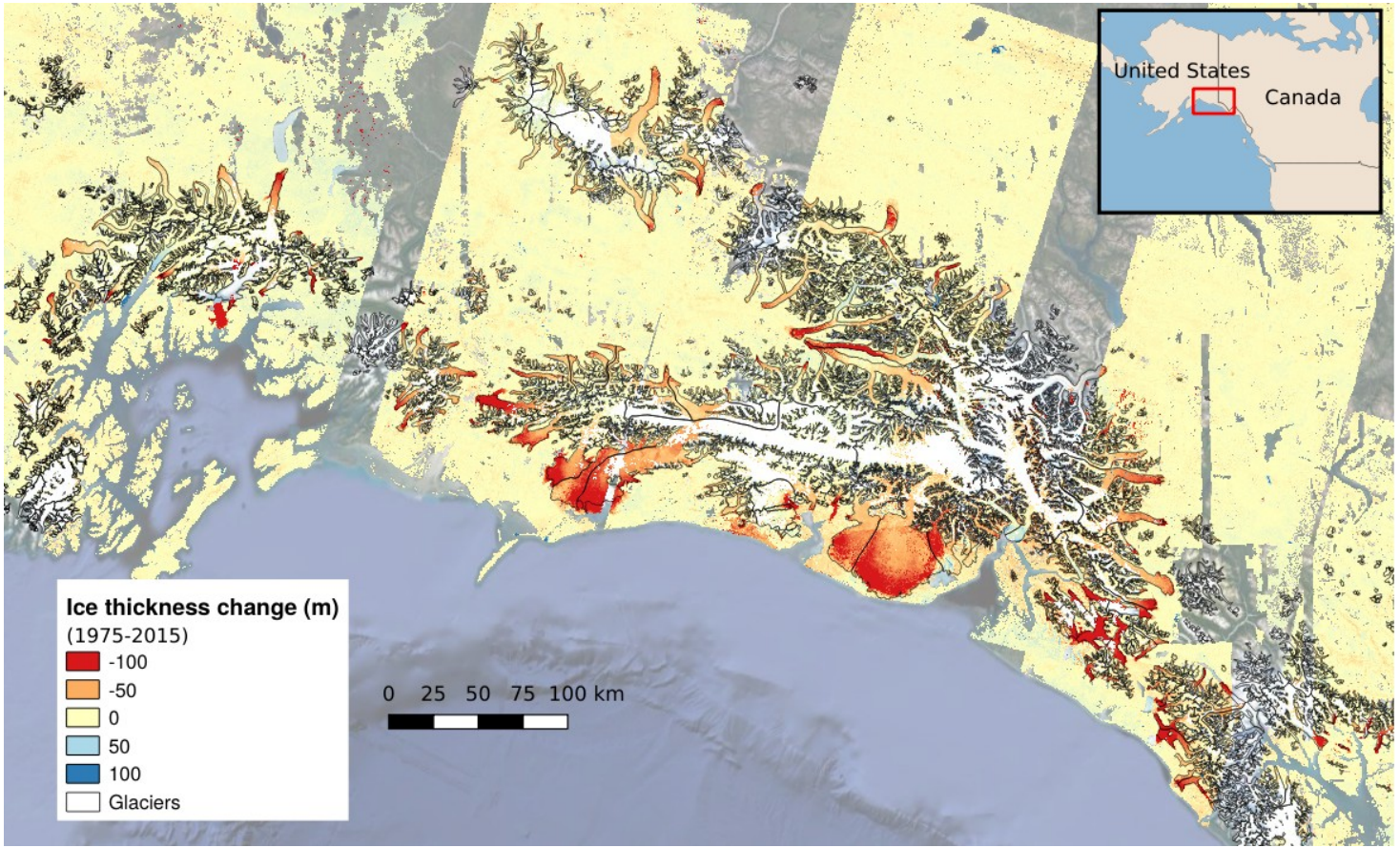

Application at regional scale - Example of the glaciers in Alaska

VI. Applications – Landslides

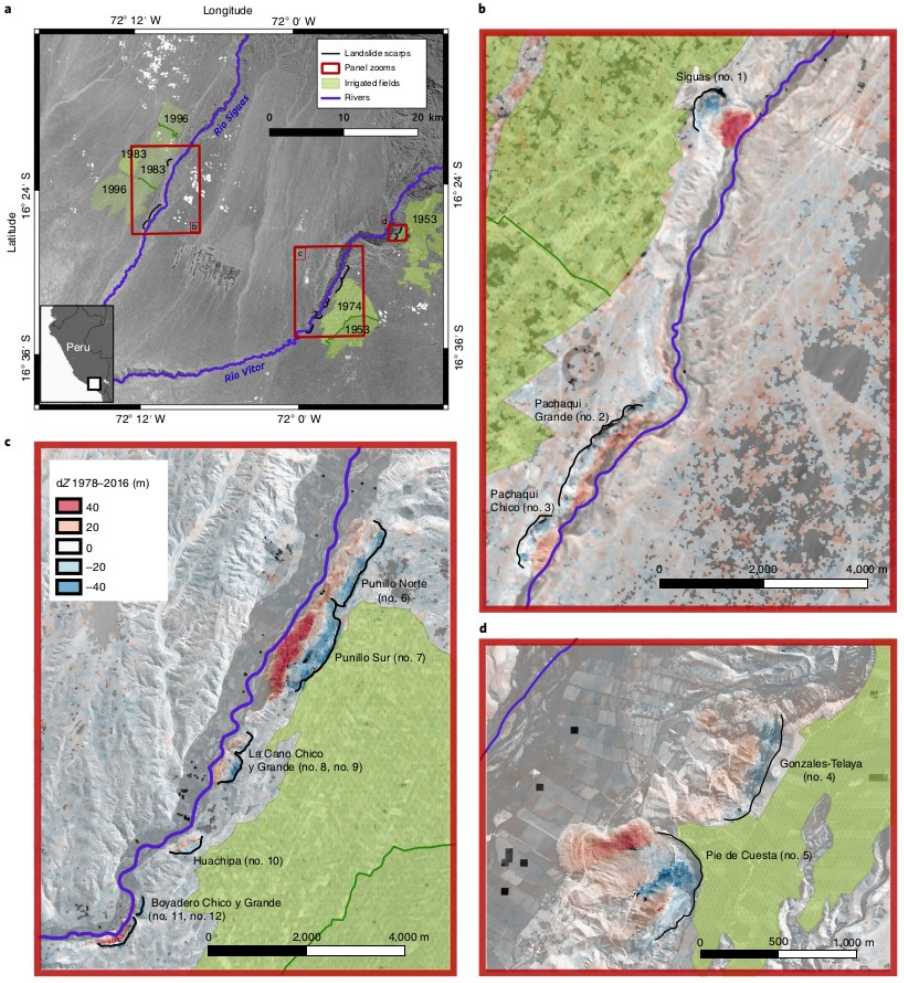

KH-9 DEMs and orthophotos have a large array of applications related to the observation of surface changes at multi-decadal scales.

- In a recent study, we observed the onset of several **mega landslides in South Peru**, by comparing KH-9 (1978) and Pléiades (2016) DEMs.
- We demonstrated that the landslides have been **triggered by the development of vast irrigation programs** in and after the 1950s.
- The DEMs were used to estimate vertical changes, while ortophotos were used to estimate the horizontal displacement.
- The long time span is key in providing surface conditions prior and after the changes.

More details in the associated paper:
Lacroix et al., 2020 (doi:10.1038/s41561-019-0500-x)

Conclusions

- We developed an **automated workflow to generate 24 m resolution DEMs** from analog KH-9 images, covering nearly all land surfaces from **1973 to 1980**.
- The workflow is able to refine camera extrisinc (position/orientation) and intrinsic (focal length, lens distortion) **without the use of manual control points**, based on an external DEM only.
- The code will be made publicly available in a few months time.
- The retrieved elevation was validated against ancilary data set and the (68% interval) **uncertainty estimated to less than 5 m vertically**.
- However, we raise particular attention to **large scale correlated biases** associated with such analog imagery, that must be taken into account when deriving volume changes.
- The KH-9 archive provides a unique opportunity to study topographic changes over decadal scales with potential applications in glaciology, seismology, natural hazards or geomorphology.

References

- Berthier, E., E. Schiefer, G. K. C. Clarke, B. Menounos, and F. Rémy. 2010. “Contribution of Alaskan Glaciers to Sea-Level Rise Derived from Satellite Imagery.” Nature Geoscience 3 (2): 92–95. https://doi.org/10.1038/ngeo737.
- Burnett, MG. 2012. Hexagon (KH-9) Mapping Camera Program and Evolution. National Reconnaissance Office (NRO), Center for the Study of National Reconnaissance (CSNR), Chantilly, VA, USA. http://refhub.elsevier.com/S0924-2716(15)00166-5/h0030.
- Ginzler, Christian, Mauro Marty, and Lars T Waser. 2019. “Landesweite digitale Vegetationshöhenmodelle aus historischen SW - Stereoluftbildern.” In Publikationen der DGPF. Vol. 28. T. P. Kersten (Ed.). https://www.dgpf.de/src/tagung/jt2019/proceedings/start.html.
- Lacroix, Pascal, Amaury Dehecq, and Edu Taipe. 2020. “Irrigation-Triggered Landslides in a Peruvian Desert Caused by Modern Intensive Farming.” Nature Geoscience 13 (1): 56–60. https://doi.org/10.1038/s41561-019-0500-x.
- Maurer, Joshua, and Summer Rupper. 2015. “Tapping into the Hexagon Spy Imagery Database: A New Automated Pipeline for Geomorphic Change Detection.” ISPRS Journal of Photogrammetry and Remote Sensing 108 (October): 113–27. https://doi.org/10.1016/j.isprsjprs.2015.06.008
- Miles, Evan S., C. Scott Watson, Fanny Brun, Etienne Berthier, Michel Esteves, Duncan J. Quincey, Katie E. Miles, Bryn Hubbard, and Patrick Wagnon. 2018. “Glacial and Geomorphic Effects of a Supraglacial Lake Drainage and Outburst Event, Everest Region, Nepal Himalaya.” The Cryosphere 12 (12): 3891–3905. https://doi.org/10.5194/tc-12-3891-2018.
- Pieczonka, Tino, Tobias Bolch, Wei Junfeng, and Liu Shiyin. 2013. “Heterogeneous Mass Loss of Glaciers in the Aksu-Tarim Catchment (Central Tien Shan) Revealed by 1976 KH-9 Hexagon and 2009 SPOT-5 Stereo Imagery.” Remote Sensing of Environment 130 (March): 233–44. https://doi.org/10.1016/j.rse.2012.11.020
- Porter, Claire, Paul Morin, Ian Howat, Myoung-Jon Noh, Brian Bates, Kenneth Peterman, Scott Keesey, et al. 2018. “ArcticDEM.” https://doi.org/10.7910/DVN/OHHUKH.
- Rizzoli, Paola, Michele Martone, Carolina Gonzalez, Christopher Wecklich, Daniela Borla Tridon, Benjamin Bräutigam, Markus Bachmann, et al. 2017. “Generation and Performance Assessment of the Global TanDEM-X Digital Elevation Model.” ISPRS Journal of Photogrammetry and Remote Sensing 132 (October): 119–39. https://doi.org/10.1016/j.isprsjprs.2017.08.008
- Shean, David E., Oleg Alexandrov, Zachary M. Moratto, Benjamin E. Smith, Ian R. Joughin, Claire Porter, and Paul Morin. 2016. “An Automated, Open-Source Pipeline for Mass Production of Digital Elevation Models (DEMs) from Very-High-Resolution Commercial Stereo Satellite Imagery.” ISPRS Journal of Photogrammetry and Remote Sensing 116 (June): 101–17. https://doi.org/10.1016/j.isprsjprs.2016.03.012.
- Surazakov, Arzhan, and Vladimir Aizen. 2010. “Positional Accuracy Evaluation of Declassified Hexagon KH-9 Mapping Camera Imagery.” Photogrammetric Engineering & Remote Sensing 76 (5): 603–8. https://doi.org/10.14358/PERS.76.5.603.